ELSEVIER

Journal of Alloys and Compounds 317–318 (2001) 141–144

Journal of ALLOYS AND COMPOUNDS

www.elsevier.com/locate/jallcom

Studies of the effect of internal and hydrostatic pressure on the structure and transport properties of $La_{2/3}Ca_{1/3}MnO_3$ thin films

G.M. Gross[a,*], R.B. Praus[a], S. Yaghoubzadeh[b], F.S. Razavi[b], H.-U. Habermeier[a]

[a]*Max-Planck Institute for Solid State Research, 70569 Stuttgart, Germany*
[b]*Department of Physics, Brock University, St. Cathrines, Canada*

Abstract

Lanthanum manganites belong to the perovskite type Mott insulators. They show a doping dependent drastic modification of conductivity including a metal–insulator transition associated with ferromagnetic ordering. We investigated $La_{2/3}Ca_{1/3}MnO_3$ thin films, a member of this class of material showing a colossal magnetoresistance. Application of internal and external pressure can be used to modify the electronic and magnetic properties of this material. It has been shown that, in $La_{2/3}Ca_{1/3}MnO_3$, as the band width for the itinerant e_g electrons broadens, it causes an enhancement of the ferromagnetic coupling and consequently an increase of the metal–insulator transition temperature T_{MI}, which is close to the ferromagnetic transition temperature T_C. Thin films were deposited on $SrTiO_3$ (STO) single crystals using the pulsed laser deposition technique. In this study we prepared films with different T_{MI} by choosing an appropriate depositing temperature, annealing condition and thickness range. We studied the effect of hydrostatic pressures on the in-situ annealed films in order to investigate the effect of external pressure on T_{MI} and resistivity as a function of annealing. Due to lattice mismatch between film and substrate we introduced controllable biaxial strain. The increase of lattice parameters and T_{MI} shows the relaxation process by varying the film thickness and by annealing thin layers. Our results are a contribution to the clarification of the interplay between the microscopic structure of Mn–O–Mn units with the macroscopic transport properties.

Keywords: Thin films; Manganites; Colossal magnetoresistance; Pressure; Annealing

1. Introduction

In manganites with chemical composition $R_{1-x}A_xMnO_3$, where R is a rare-earth and A a divalent ion, the Mn sites are occupied by Mn^{3+} and Mn^{4+} ions; their relative density is determined by the concentration of the A atoms in order to ensure charge neutrality. The system undergoes, at a critical hole concentration, a metal–insulator (MI) transition at T_{MI}, and becomes a ferromagnetic metal for $T < T_{MI}$ [1]. These materials have recently attracted scientific and technological interest due to the occurrence of a colossal magnetoresistance (CMR), charge and orbital ordering and various magnetic phenomena [2]. The physical properties are in close relation to the complex lattice-charge coupling and are sensitive to temperature, pressure, magnetic field and hole concentration [3]. Ferromagnetic ordering has been observed in the La–Ca–Mn–O system in a hole density range of $0.2 < x < 0.5$ in close relation with metallic conductivity [4]. Based on the double exchange theory, the electronic transport is qualitatively explained by charge transfer between Mn^{3+}–O–Mn^{4+} ions, and is thus strongly influenced by the Mn–O–Mn bond length and bond angle [5]. Recently, it has been suggested that a qualitative explanation needs a contribution from the Jahn–Teller effect resulting in a strong electron–phonon coupling [6].

In this paper we study systematically the role of a thickness dependent epitaxial strain affecting the transport and magnetotransport properties of LCMO thin films. Hydrostatic pressure superimposed on this strain is used to reversibly reduce the biaxial strain. Thus an avenue to controllably investigate the role of the microscopic dimensions of the Mn–O–Mn building block is paved.

2. Experimental

Films of $La_{2/3}Ca_{1/3}MnO_3$ were prepared by the pulsed laser deposition technique on (100) $SrTiO_3$ single crystal substrates using a KrF eximer laser with $\lambda = 248$ nm. Thin layers in the thickness range 40–500 nm were prepared at 800°C and an oxygen pressure of 40 Pa. After deposition,

*Corresponding author.

0925-8388/01/$ – see front matter
PII: S0925-8388(00)01335-9

samples were annealed in situ for 1 h at 780°C in 10^5 Pa of flowing oxygen. Further details are given elsewhere [7].

In order to reduce growth-induced stress, the films were subjected to an annealing process at 900°C in 10^5 Pa of flowing oxygen for 1 h. The magnetic and transport properties of the films were measured before and after annealing by standard techniques. Structural information on the LCMO films were obtained by X-ray diffraction.

A second set of samples were deposited with an XeCl eximer laser with $\lambda = 308$ nm [8]. Films with a thickness of about 85 nm were prepared and one part was annealed in situ at 750°C, and another at 900°C. We applied hydrostatic pressure and investigated the transport properties.

3. Results

In this case study, experiments were confined to the chemical composition of $La_{2/3}Ca_{1/3}MnO_3$. We fixed the Mn^{3+} to Mn^{4+} ratio by the amount of calcium.

The films were single phase and grown epitaxially on single crystal STO as indicated by the (111) pole figure exhibiting only a four-fold symmetry of the film maxima. Further X-ray diffraction investigations of the out-of-plane lattice parameter c of the films were performed with Θ–2Θ geometry using the substrate as an internal standard. Profile analysis results in a reliability $R < 6\%$ using a convolution of the Gaussian and Lorentz function. After deposition we determined the out-of-plane lattice parameter which increases with film thickness. The annealing step at 900°C results in a further increase due to further relaxation of the tensile epitaxial strain in the films (Fig. 1a).

The transport properties of the films were studied from 5 K up to 350 K by applying a current of $I = 100$ μA. Analysis of the $\rho(T)$ measurements shows a distinct dependence of the metal–insulator transition temperature T_{MI} on film thickness. For 40 nm thick films, a T_{MI} of about 200 K was measured, which rises to 260 K for a 300 nm film. In the thickness range up to 100 nm the increase of T_{MI} is rather steep (Fig. 1b) and then flattens. T_{MI} shifts to higher temperatures and approaches the bulk value of $T = 275$ K for thick films after post-annealing (Fig. 1b, Fig. 2a). As can be seen from Fig. 2b the resistivity of the thin films decreases tremendously upon post-annealing; thick films, however, show a slight modification of resistivity only (Fig. 2a).

The magnetoresistance (MR) ($[R(0) - R(H)/R(H)] \times 100\%$) increases with the strength of the magnetic field applied parallel to the film plane. Furthermore, we found a thickness and annealing dependence. Fig. 3a,b shows the magnetoresistance as a function of temperature for a 40 nm and 300 nm film, respectively. For the thin film, the magnetoresistance versus temperature is characterized by a double peak structure for the as-grown state. Upon annealing, a single peak appears at a much higher temperature (Fig. 3b). The thick film (Fig. 3a) has a single peak in the as-grown state appearing at 260 K which shifts to 275 K after annealing.

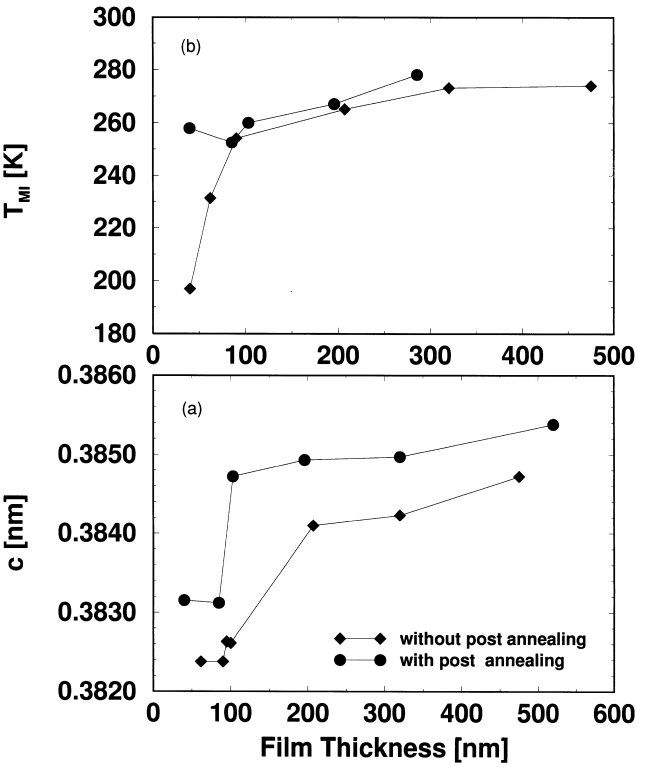

Fig. 1. The out-of-plane lattice parameter c (a) and metal–insulator transition temperature T_{MI} (b) increase by thermal annealing.

With increasing film thickness the peak maximum decreases and the $MR(T)$ curve becomes narrow and shifts to higher temperatures (Fig. 3a,b). This development of the T_{MI} and $MR(T)$ curve with thickness undergoes a strong enhancement through post-annealing. Comparing the results of the lattice parameter measurements and the increase of T_{MI} with film thickness and after post-annealing, we see a correlation between the curves (Fig. 1a,b).

Magnetization measurements show qualitatively the same dependence on film thickness and post-annealing for the remanent magnetization M_R and saturation magnetization M_S. M_S of 3.0 and 3.1 μ_B, close to the expected bulk value of 3.3 μ_B, were determined before and after annealing, respectively, in samples with $d = 290$ nm. The remanent magnetization M_R also increases with thickness.

The temperature dependence of the resistivity under hydrostatic pressure is shown in Fig. 4a,b. We investigated films with an identical thickness of about 85 nm, but annealed in situ at two different temperatures, $T_1 = 750$°C and $T_2 = 900$°C. Both results show that the resistivity decreases similar to the effect of an applied magnetic field and T_{MI} shifts to higher temperatures. This effect is much more pronounced for thin films annealed at 750°C. Films already exhibiting ordering temperatures near the bulk

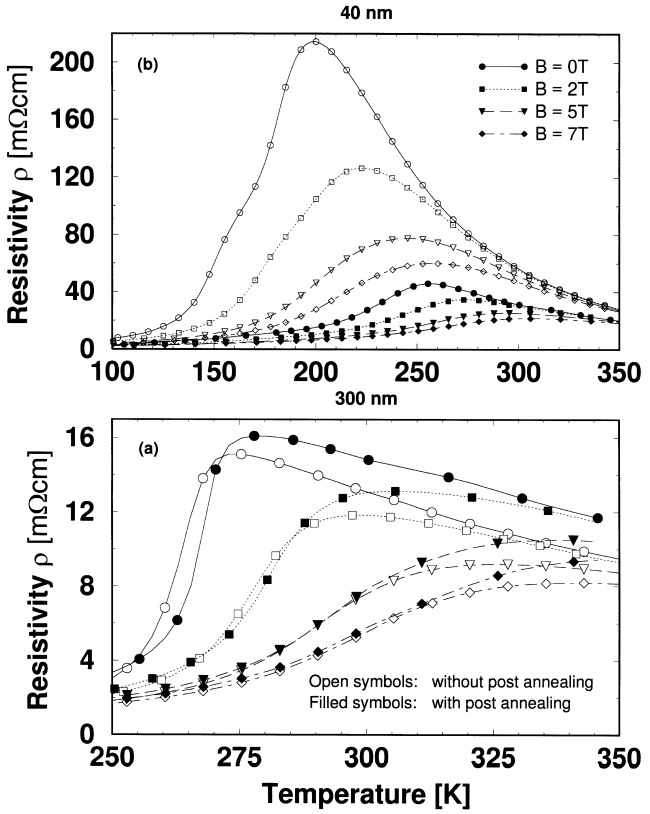

Fig. 2. Resistivity as a function of temperature and applied magnetic field for films with a thickness of 300 nm (a) and 40 nm (b). Open symbols, before annealing; filled symbols, after annealing.

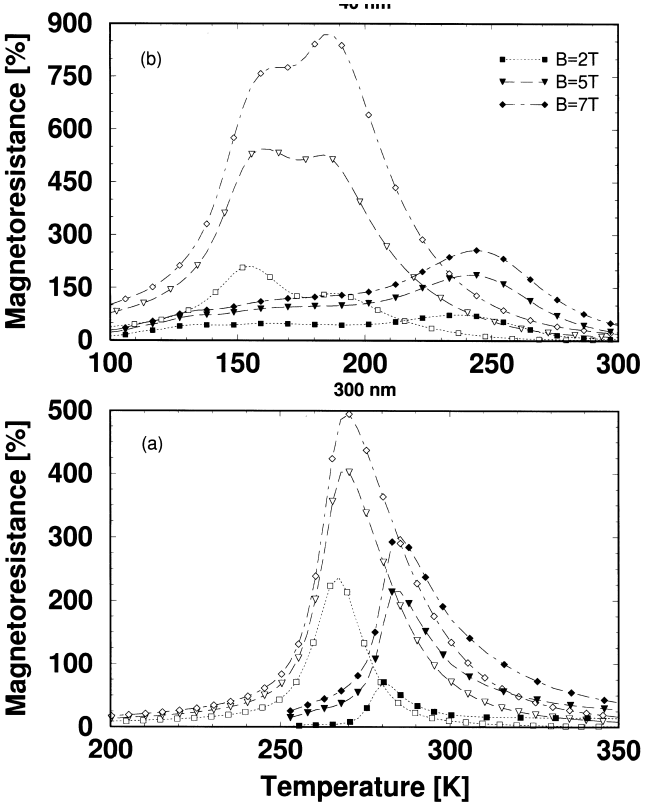

Fig. 3. Magnetoresistance as a function of temperature and applied magnetic field for films with a thickness of 300 nm (a) and 40 nm (b). Open symbols, before annealing; filled symbols, after annealing.

value after annealing at 900°C show no large effect with increasing hydrostatic pressure. The increase of pressure is associated with an increase of the transition temperature, which can be interpreted as being a consequence of pressure-induced contraction and alignment of the Mn–O–Mn bonds. The same effect was determined in the $PrNiO_3$ perovskite structure by neutron diffraction measurements under pressure [9].

The experimental results presented in this paper can self-consistently be interpreted by the following qualitative model. The films grow pseudomorphically on the STO substrate up to a thickness of about 100 nm, thus being under homogeneous tensile epitaxial strain. The strain causes an elongation of the Mn–O–Mn bond length and thus reduces the charge transfer according to the double exchange model. A consequence of the tensile strain is a reduced T_{MI} and reduced peak temperature for the magnetoresistance. Tentatively, the double peak structure of magnetoresistance versus temperature is ascribed to a strain-induced splitting into two slightly different crystallographic phases. Upon annealing, this biaxial epitaxial strain relaxes and the films show properties similar to the bulk material.

In thick films (~200–300 nm) an intrinsic strain relaxation mechanism occurs. The majority of the volume is strain lean or even strain free, thus post-deposition annealing causes a small enhancement of T_{MI} and a peak in MR versus T.

The superimposed hydrostatic pressure reduces the effect of the epitaxial strain, consequently the lower temperature annealed strained film ($T = 750$°C) shows a much more pronounced effect than the film annealed at 900°C.

4. Conclusion

We reproducibly deposited thin films of $La_{2/3}Ca_{1/3}MnO_3$ with various thicknesses using pulsed laser deposition, systematically inducing biaxial strain. We detected a correlation between the lattice parameters, resistivity ρ, the metal–insulator transition temperature T_{MI}, heat treatment and the applied hydrostatic pressure.

The T_{MI} is shifted towards higher temperatures, approaching the bulk value in thick and post-annealed films. Thin films with $d < 100$ nm are strongly effected by post-annealing, as demonstrated by the decrease in resistivity and increase of the out-of-plane lattice parameter.

For films with $T_{MI} < 250$, K the e_g band width increases rapidly with annealing and applied pressure, causing the resistivity to decrease quickly as pressure increases or samples are post-annealed. However, for films with $T_{MI} >$

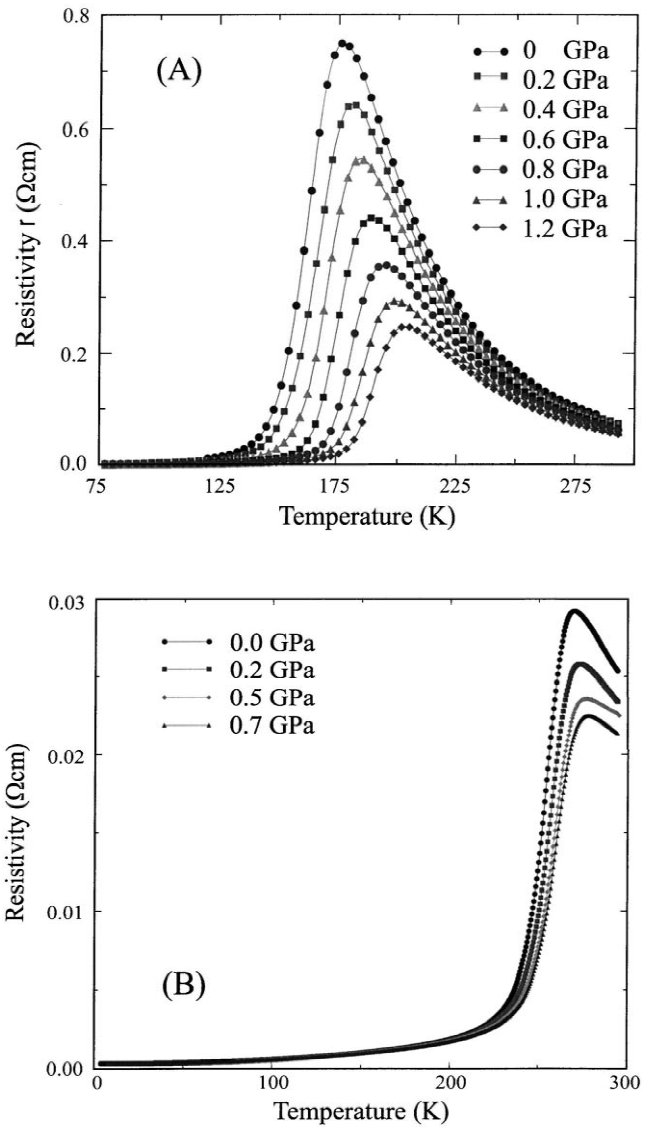

Fig. 4. Temperature dependence of the resistivity (T) under various pressures. Both films have identical thicknesses, but were annealed at 750°C (a) and 900°C (b).

250 K, other mechanisms, possibly a change in the electron–phonon interaction, are involved in causing $La_{2/3}Ca_{1/3}MnO_3$ to become more metallic as the pressure increases.

References

[1] S. Jin, T.H. Tiefel, M. McCormack, R. Fastnacht, R. Ramesh, L.H. Chen, Science 264 (1994) 413.
[2] A.P. Ramirez, S.-W. Cheong, P. Schiffer, J. Appl. Phys. 81 (1997) 5337.
[3] P.G. Radaelli, G. Iannone, M. Marezio, H.Y. Hwang, S.-W. Cheong, J.D. Jorgensen, D.N. Argyriou, Phys. Rev. B 56 (1997) 8265.
[4] A.J. Millis, Nature 392 (1998) 147.
[5] C. Zener, Phys. Rev. 82 (1995) 403.
[6] A.J. Millis, P.B. Littlewood, B.I. Shraiman, Phys. Rev. Lett. 74 (1995) 5144.
[7] R. Praus, B. Leibold, G.M. Gross, H.-U. Habermeier, Appl. Surf. Sci. 138/139 (1999) 40.
[8] T. Roch, S. Yaghoubzadeh, F.S. Razavi, B. Leibold, R. Praus, H.-U. Habermeier, Appl. Phys. A 67 (1998) 723.
[9] M. Medarele, J. Mesot, P. Lacorre, S. Rosenkranzm, P. Fischer, K. Gobrecht, Phys. Rev. B 52 (1995) 9248.